Synthetic Metals 190 (2014) 1–7

Contents lists available at ScienceDirect

Synthetic Metals

journal homepage: www.elsevier.com/locate/synmet

White polymer light emitting diode materials introducing dendritic quinoxaline derivative: Synthesis, optical and electroluminescent properties

Ho Jun Song[a,b], Gyo Jic Shin[b], Kyung Ho Choi[b], Sangkug Lee[b], Doo Kyung Moon[a,*]

[a] Department of Materials Chemistry and Engineering, Konkuk University, 1 Hwayang-dong, Gwangjin-gu, Seoul 143-701, Republic of Korea
[b] Cungcheong Regional Division IT Convergence Material R&D Group, Korea Institute of Industrial Technology, 89 Yangdaegiro-gil, Ipjang-myeon, Seobuk-gu, Cheonan-si, Chungcheongnam-do 331-822, Republic of Korea

ARTICLE INFO

Article history:
Received 18 November 2013
Received in revised form 3 January 2014
Accepted 7 January 2014
Available online 13 February 2014

Keywords:
Dendritic derivative
Quinoxaline
Conjugated polymer
WPLED

ABSTRACT

Copolymers including dendritic-quinoxaline (DTQ1G, DTQ2G) (<0.1 mol%) as dopant derivative have been synthesized on a polyfluorene (PF) backbone based on the Suzuki coupling reaction. The UV–vis spectra of polymers showed similar behaviors in the solution and on the film. However, PL spectra were similar to that of PF in solution, but the peak around 590 nm increased as the amounts of DTQ1G and DTQ2G were increased in the casting film. In thin film, the intensities of the dendritic TQ monomers increased with the generation number of the dendrons. In case of PFDTQ2G03, the luminous efficiency and power efficiency were 0.66 cd/A and 0.29 lm/W, respectively with a maximum brightness of 3792 cd/m^2. The CIE coordinates of PFDTQ1G05 and PFDTQ2G10 were (0.33, 0.30) and (0.35, 0.34) close to the pure white coordinates of (0.33, 0.33).

1. Introduction

For the past decades, π-conjugated polymer has been applied to diverse applications such as organic light-emitting diodes (OLEDs) [1–6], organic photovoltaic cells (OPVs) [7–9], organic thin-film transistors (OTFTs) [10–12], and liquid crystal application (LC) [13]. In particular, polymer light-emitting diodes (PLED) present advantages in large-area fabrication methods, such as ink-jet and screen printing with solution processes. As a result, the material has drawn great attention as a next-generation material to replace vacuum deposition with small molecules. Thanks to its convenience and flexibility, polymer film has been popular in the flexible display sector [8,14].

A number of studies have been focusing on PLED materials in various colors since the development of poly(phenylenevinylene) in 1990 [15]. It has been reported that polyfluorene (PF) [16], poly(phenylenevinylene) (PPV) [17], and poly(methoxy, ethylhexyloxy phenylenevinylene) (MEH-PPV) [18] are the representative blue-emitting, green-emitting, and orange and red-emitting materials, respectively. Full-color displays have been enabled by such polymers [4,8].

Recently, there have been more studies on white polymer light-emitting diodes (WPLED) that introduced diverse chromophores to the blue emitting material, PF. If chromophore is introduced to a PF backbone, aggregation and excimers are suppressed. As a result, effective energy transfer occurs in such materials. Therefore, high-efficiency WPLEDs can be realized [19,20]. Recently, we introduced a small amount of low-band-gap chromophore (<0.3 mol%) to a PF backbone and had it copolymerized. Depending on the dopant mol ratio, various color changes (white, green, yellow, etc.) could be detected with high efficiency [5].

The electron-deficient quinoxaline derivative is a leading orange-emitting chromophore. Due to thermal and electrochemical stability and high PL and EL efficiency, the quinoxaline derivative has been widely used in white and orange light-emitting polymers [21–23]. In addition, the quinoxaline derivative can be easily tuned in structure with high solubility. Therefore, electronic characteristics can be changed by introducing various substituents [24,25].

Recently, there have been many studies on the introduction of dendritic derivative, which has superior quantum efficiency characteristics because dendritic derivative reduce the formation of excimers and the aggregation of emitters [26]. The dendrons not only protect the polymer rods from both aggregation and degradation but also improve PL quantum yields [27]. Therefore, if the dendritic derivative is introduced to the quinoxaline derivative, emitter may show effective emitting property.

* Corresponding author. Tel.: +82 2 450 3498; fax: +82 2 444 0765.
E-mail address: dkmoon@konkuk.ac.kr (D.K. Moon).

0379-6779/$ – see front matter © 2014 Elsevier B.V. All rights reserved.
http://dx.doi.org/10.1016/j.synthmet.2014.01.019

In this study, 0.03–0.1 mol% of dendritic quinoxaline derivative was adopted as dopant with an orange emitter and PF as a host. To improve PL quantum yields and aggregation of emitters, the dendritic quinoxaline derivative was introduced to the PF backbone. The Forster energy transfer was investigated, as well as the charge trapping and charge balance effects between host and dopant, and the optimum mol concentration for effective white-emitting polymer was realized.

2. Experiment

2.1. Instruments and characterization

Unless otherwise specified, all the reactions were carried out under nitrogen atmosphere. Solvents were dried by standard procedures. Column chromatography was performed with the use of silica gel (230–400 mesh, Merck) as the stationary phase. ^{1}H NMR spectra were performed in a Bruker ARX 400 spectrometer using solutions in $CDCl_3$, and chemical concentrations were recorded in units of ppm with TMS as the internal standard. Electronic absorption spectra were measured in chloroform using a HP Agilent 8453 UV–vis spectrophotometer. Photoluminescent spectra were recorded by a Perkin Elmer LS 55 luminescence spectrometer. Cyclic voltammetry experiments were performed with a Zahner IM6eX Potentionstat/Galvanostat. All measurements were carried out at room temperature with a conventional three-electrode configuration consisting of platinum working and auxiliary electrodes and a nonaqueous Ag/AgCl reference electrode at the scan rate of 50 mV/s. The solvent in all experiments was acetonitrile and the supporting electrolyte was 0.1 M tetrabutyl ammonium-tetrafluoroborate. TGA measurements were performed on a NETZSCH TG 209 F3 thermogravimetric analyzer. All GPC analyses were made by using THF as the eluant and polystyrene standard as the reference.

2.2. EL device fabrication and characterization

The fabricated device structure was ITO/PEDOT:PSS/polymer/BaF_2/Ba/Al. All of the polymer light-emitting diodes were prepared using the following device fabrication procedure. Glass/indium tin oxide (ITO) substrates [Sanyo, Japan (10 Ω/γ)] were sequentially patterned lithographically, cleaned with detergent, and ultrasonicated in deionized water, acetone and isopropyl alcohol. Then, the substrates were dried on a hotplate at 120 °C for 10 min and treated with oxygen plasma for 10 min in order to improve the contact angle just before the film coating process. Poly(3,4-ethylene-dioxythiophene):poly(styrene-sulfonate) (PEDOT:PSS, Baytron P 4083 Bayer AG) was passed through a 0.45-μm filter before being deposited onto ITO at a thickness of ca. 32 nm through spin-coating at 4000 rpm in air, and then dried at 120 °C for 20 min inside a glove box. The light-emitting polymer layer was then deposited onto the film by spin coating a polymer solution in chlorobenzene (1.5 wt.%) at a speed of 1000 rpm for 30 s on top of the PEDOT:PSS layer. The device was thermally annealed at 90 °C for 30 min in a glove box. The device fabrication was completed by depositing thin layers of BaF_2 (1 nm), Ba (2 nm) and Al (200 nm) at pressures less than 10^{-6} Torr. The active area of the device was 9.0 mm^2. Finally, the cell was encapsulated using UV-curing glue (Nagase, Japan). EL spectra, Commission Internationale de l'Eclairage (CIE) coordinates, current–voltage, and brightness–voltage characteristics of devices were measured with a Spectrascan PR670 spectrophotometer in the forward direction, and a computer-controlled Keithley 2400 under ambient conditions.

2.3. Materials and synthesis of monomers

All reagents were purchased from Aldrich, Acros or TCI companies. All chemicals were used without further purification. The following compounds were synthesized following modified literature procedures: 4,4′-(5,8-bis(5-bromothiophen-2-yl)quinoxaline-2,3-diyl)diphenol [28], (5-(bromomethyl)-1,3-phenylene)bis(oxy)bis(methylene)dibenzene and (5,5′-(5-(bromomethyl)-1,3-phenylene)bis(oxy)bis(methylene)bis(benzene-5,3,1-triyl))tetrakis(oxy)tetrakis(methylene)tetrabenzene [29].

2.3.1. Synthesis of 2,3-bis(4-(3,5-bis(benzyloxy)benzyloxy)phenyl)-5,8-bis(5-bromothiophen-2-yl)quinoxaline (DTQ1G)

4,4′-(5,8-bis(5-Bromothiophen-2-yl)quinoxaline-2,3-diyl)diphenol (0.2 g, 0.31 mmol), (5-(bromomethyl)-1,3-phenylene) bis(oxy)bis(methylene)dibenzene (0.3 g, 0.78 mmol), K_2CO_3 (0.43 g, 3.13 mmol), and N,N-dimethylformamide (DMF) (15 mL) were placed in a 250 mL two-neck round-bottom flask, and then, this mixture was stirred at 90 °C for 24 h. The reaction mixture was extracted using chloroform/brine, and then, the organic layer was separated and concentrated. The product was purified using column chromatography using dichloromethane as the eluent. The product yield was 49% (0.19 g). ^{1}H NMR (400 MHz; $CDCl_3$; Me_4Si): 8.03 (t, 2H), 7.85 (d, 1H), 7.66 (t, 4H), 7.57 (t, 2H) 7.42–7.29 (m, 20H) 7.18 (d, 1H) 6.98 (t, 4H) 6.70 (s, 4H) 6.58 (s, 2H) 5.04 (s, 12H). Anal. Calcd. for: $C_{70}H_{52}Br_2N_2O_6S_2$: C, 67.74; H, 4.22; N, 2.26; O, 7.73; S, 5.17. Found: C, 72.36; H, 4.53; N, 2.45; O, 8.94; S, 5.63.

2.3.2. Synthesis of 2,3-bis(4-(3,5-bis(3,5-bis(benzyloxy)benzyloxy)benzyloxy)phenyl)-5,8-bis(5-bromothiophen-2-yl)quinoxaline (DTQ2G)

4,4′-(5,8-bis(5-Bromothiophen-2-yl)quinoxaline-2,3-diyl)diphenol (0.3 g, 0.46 mmol), (5,5′-(5-(bromomethyl)-1,3-phenylene) bis(oxy)bis(methylene)bis(benzene-5,3,1-triyl))tetrakis(oxy)tetrakis(methylene)tetrabenzene (0.94 g, 1.17 mmol), K_2CO_3 (0.64 g, 4.69 mmol), and N,N-dimethylformamide (DMF) (15 mL) were placed in a 250 mL two-neck round-bottom flask, and then, this mixture was stirred at 90 °C for 24 h. The reaction mixture was extracted using chloroform/brine, and then, the organic layer was separated and concentrated. The product was purified using column chromatography using dichloromethane as the eluent. The product yield was 32% (0.31 g). ^{1}H NMR (400 MHz; $CDCl_3$; Me_4Si): 8.04 (t, 2H), 7.85 (d, 1H), 7.67 (t, 4H), 7.58 (t, 2H) 7.38–7.28 (m, 40H) 7.18 (d, 1H) 7.00 (t, 4H) 6.66 (s, 12H) 6.54 (s, 6H) 4.99 (s, 28H). Anal. Calcd. for: $C_{126}H_{100}Br_2N_2O_{14}S_2$: C, 72.41; H, 4.82; N, 1.34; O, 10.72; S, 3.07. Found: C, 74.88; H, 4.94; N, 1.41; O, 11.56; S, 3.18.

2.4. Polymerization

Reaction monomers, $(PPh_3)_4Pd(0)$ (1.5 mol%) and Aliquat 336 were dissolved in a mixture of toluene and an aqueous solution of 2 M K_2CO_3. The solution was refluxed for 72 h with vigorous stirring in nitrogen atmosphere, and then excess amounts of bromobenzene, as an end capper, were added and stirring continued for 12 h. The whole mixture was poured into methanol. The precipitate was filtered off, and purified with methanol, acetone, hexane, chloroform in soxhlet.

2.4.1. PFDTQ1G03

9,9-Dioctylfluorene-2,7-dibromofluorene (0.499 equiv.), 2,2′-(9,9-dioctyl-9H-fluorene-2,7-diyl)bis(4,4,5,5-tetramethyl-1,3,2-dioxaborolane) (0.5 equiv.), 3-bis(4-(3,5-bis(benzyloxy)benzyloxy)phenyl)-5,8-bis(5-bromothiophen-2-yl)quinoxaline (*DTQ1G*) (0.0003 equiv.); Yield: 0.16 g (38%); ^{1}H NMR (400 MHz; $CDCl_3$;

Me_4Si): δ = 7.85–7.83 (m), 7.73–7.28 (m), 2.14 (m), 1.22–1.15 (m), 0.85–0.72 (m).

2.4.2. PFDTQ1G05

9,9-Dioctylfluorene-2,7-dibromofluorene (0.499 equiv.), 2,2′-(9,9-dioctyl-9H-fluorene-2,7-diyl)bis(4,4,5,5-tetramethyl-1,3,2-dioxaborolane) (0.5 equiv.), 3-bis(4-(3,5-bis(benzyloxy)benzyloxy) phenyl)-5,8-bis(5-bromothiophen-2-yl)quinoxaline (*DTQ1G*) (0.0005 equiv.); Yield: 0.28 g (66%); ^{1}H NMR (400 MHz; $CDCl_3$; Me_4Si): δ = 7.87–7.85 (m), 7.73–7.28 (m), 2.14 (m), 1.22–1.15 (m), 0.85–0.82 (m).

2.4.3. PFDTQ1G10

9,9-Dioctylfluorene-2,7-dibromofluorene (0.499 equiv.), 2,2′-(9,9-dioctyl-9H-fluorene-2,7-diyl)bis(4,4,5,5-tetramethyl-1,3,2-dioxaborolane) (0.5 equiv.), 3-bis(4-(3,5-bis(benzyloxy)benzyloxy) phenyl)-5,8-bis(5-bromothiophen-2-yl)quinoxaline (*DTQ1G*) (0.001 equiv.); Yield: 0.30 g (71%); ^{1}H NMR (400 MHz; $CDCl_3$; Me_4Si): δ = 7.87–7.85 (m), 7.73–7.28 (m), 2.14 (m), 1.27–1.15 (m), 0.85–0.81 (m).

2.4.4. PFDTQ2G03

9,9-Dioctylfluorene-2,7-dibromofluorene (0.499 equiv.), 2,2′-(9,9-dioctyl-9H-fluorene-2,7-diyl)bis(4,4,5,5-tetramethyl-1,3,2-dioxaborolane) (0.5 equiv.), 2,3-bis(4-(3,5-bis(3,5-bis(benzyloxy) benzyloxy)benzyloxy)phenyl)-5,8-bis(5-bromothiophen-2-yl)quinoxaline (*DTQ2G*) (0.0003 equiv.); Yield: 0.28 g (66%); ^{1}H NMR (400 MHz; $CDCl_3$; Me_4Si): δ = 7.87–7.85 (m), 7.73–7.28 (m), 2.14 (m), 1.22–1.15 (m), 0.85–0.81 (m).

2.4.5. PFDTQ2G05

9,9-Dioctylfluorene-2,7-dibromofluorene (0.499 equiv.), 2,2′-(9,9-dioctyl-9H-fluorene-2,7-diyl)bis(4,4,5,5-tetramethyl-1,3,2-dioxaborolane) (0.5 equiv.), 2,3-bis(4-(3,5-bis(3,5-bis(benzyloxy)benzyloxy)benzyloxy)phenyl)-5,8-bis(5-bromothiophen-2-yl) quinoxaline (*DTQ2G*) (0.0005 equiv.); Yield: 0.22 g (52%); ^{1}H NMR (400 MHz; $CDCl_3$; Me_4Si): δ = 7.87–7.85 (m), 7.73–7.28 (m), 2.14 (m), 1.22–1.15 (m), 0.85–0.81 (m).

2.4.6. PFDTQ2G10

9,9-Dioctylfluorene-2,7-dibromofluorene (0.499 equiv.), 2,2′-(9,9-dioctyl-9H-fluorene-2,7-diyl)bis(4,4,5,5-tetramethyl-1,3,2-dioxaborolane) (0.5 equiv.), 2,3-bis(4-(3,5-bis(3,5-bis(benzyloxy) benzyloxy)benzyloxy)phenyl)-5,8-bis(5-bromothiophen-2-yl)quinoxaline (*DTQ2G*) (0.001 equiv.); Yield: 0.27 g (64%); ^{1}H NMR (400 MHz; $CDCl_3$; Me_4Si): δ = 7.85–7.83 (m), 7.73–7.28 (m), 2.14 (m), 1.22–1.15 (m), 0.85–0.81 (m).

3. Results and discussion

3.1. Synthesis and characterization of the polymers

As shown in Scheme 1, a total of 6 polymers were polymerized through Suzuki coupling reaction by using different mol ratios (monomers DTQ1G and DTQ2G) with 38–71% yield ratio. The polymerization was reacted at 90 °C for 72 h with palladium catalyst (0) and 2 M potassium carbonate solution. In addition, aliquot 336 and toluene were used as surfactant and solvent, respectively. Once the polymerization was completed, it was end-capped with bromobenzene. All polymers were purified with soxhlet in order of methanol, acetone and chloroform, and the chloroform fraction was recovered. All polymers dissolved in general organic solvents such as THF, chloroform, chlorobenzene and dichlorobenzene, and a homogenous and transparent film has been formed through spin-coating.

In the H NMR spectra obtained (see Figure S1), an aromatic peak was found at 7.0–8.0 ppm, while a proton peak originating from an aliphatic peak was detected at 0.8–5.0 ppm. A proton peak from the small amount (10^{-4} mol against total monomer) of the dopant (DTQ1G, DTQ2G) was not observed. As shown in the references, the actual dopant ratio could not be measured through NMR, FT-IR or elemental analysis against the dopant ratio 0.5 mol% or below [5,30]. As shown in Table 1, according to the measurement of GPC

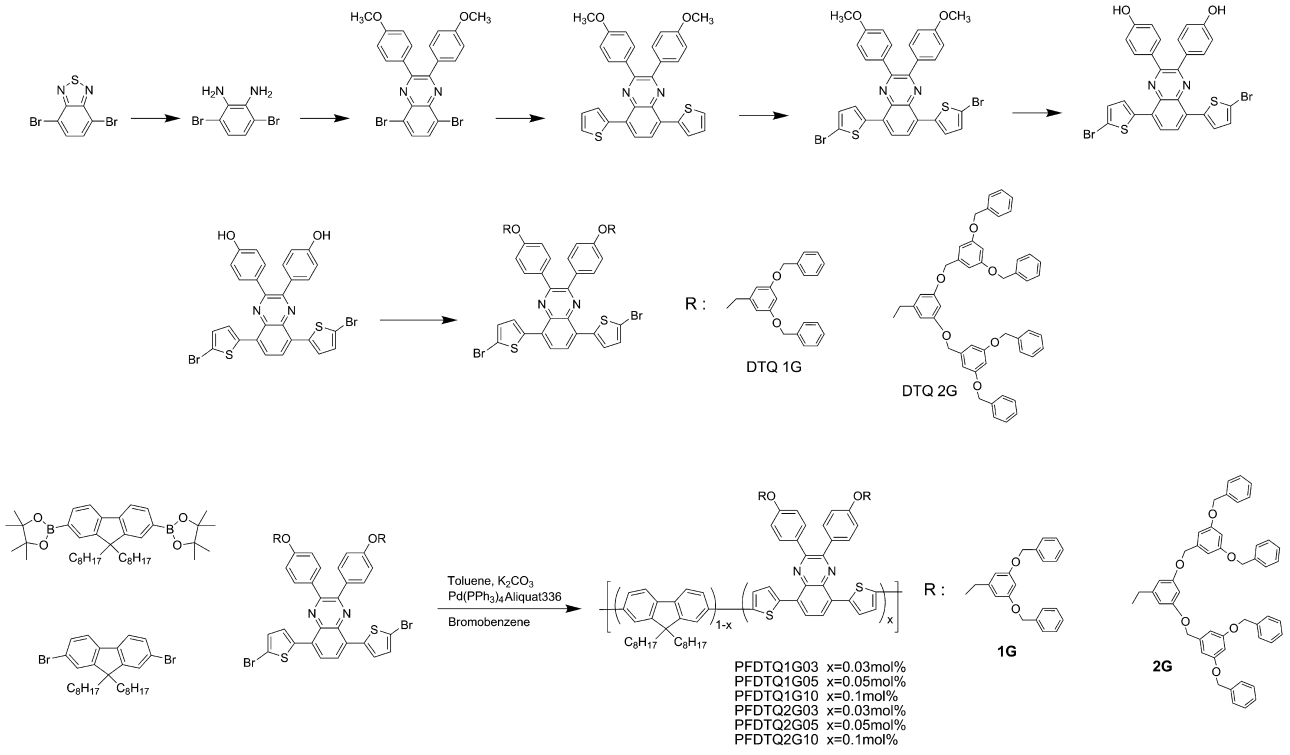

Scheme 1. Monomer synthesis and polymerization.

Table 1
Physical properties of the polymers.

Polymer	M_n (kg/mol)	M_w (kg/mol)	PDI	T_d [a] (°C)	Φ_{PL} [b]
PFDTQ1G03	15.9	18.5	1.68	414	0.77
PFDTQ1G05	15.6	36.4	2.32	420	0.79
PFDTQ1G10	16.6	38.6	2.31	419	0.72
PFDTQ2G03	14.8	33.6	2.26	407	0.78
PFDTQ2G05	14.9	35.9	2.39	415	0.77
PFDTQ2G10	16.1	38.7	2.40	411	0.73

[a] Temperature resulting in 5% weight loss based on initial weight.
[b] Solution fluorescence quantum yields measured in chloroform relative to polyfluorene (ca. 1×10^{-5} M, $\Phi_{PL} = 0.79$) in chloroform as a standard.

with polystyrene as the standard, the number average molecular weight of all polymers ranged from 12,500 to 26,000. The degree of polymerization was similar to that of general EL polymer [5]. The polydispersity indices (PDI) showed a very narrow distribution (1.68–2.04).

Thermal analysis through TGA (see Figure S2) indicated high thermal stability (around 400°) at 5 wt% loss, which reveals applicability to display application sectors in which high thermal stability (400 °C or higher) is required [5,31]. In addition, thermal characteristics similar to PF were found in all polymers, which mean that the dopant derivatives introduced to the PF backbone had no effect on polymer rigidity. The weight loss of 45–50% at 400–500 °C is the result of the degradation of the skeletal PF backbone chain structure. The PF backbone is decomposed to oligomers or other short chain structures [32].

4. Optical and electrochemical properties

Fig. 1 reveals the UV–vis spectra and PL spectra of all polymer films. For film state, the absorption spectra of all polymers were broad in comparison with those of the solution (see Figure S3a)). This kind of result was because the dihedral angle between fluorene rings in the thin film is considered to decrease due to stronger interchain interaction [32–34]. The absorption peak of the TQ derivative (dopant) was not observed because of the small amount of dopant used. In case of PL spectra, as shown in Fig. 1b), as DTQ content increased, the 590 nm emission peak broadened, unlike for the solution, because of increases in the intermolecular interaction among the polymer main chains [19].

Fig. 2 shows the PL spectra of dendritic TQ monomers in solution (10^{-5} M) and films (drop cast in same mol ratio). In solution, as shown in Fig. 2, the intensities of the dendritic TQ monomers were similar. Whereas, in thin film, the intensities of the dendritic TQ monomers increased with the generation number of the dendrons, which are attributed to the peripheral bulky dendron units. The emission intensity of DTQ2G increased by 10 times compared to that of DTQ without dendritic unit, which may be due to dendritic substitute that can efficiently decrease the fluorescence quenching induced by self-absorption and excimer emission [35].

According to the comparison between the UV–vis spectrum of DTQ1G, DTQ2G and PL spectra of PF (see Figure S4), the absorption spectra of DTQ1G and DTQ2G derivative were overlapped in the PL spectra of PF, which means effective absorption of PF emission energy by TQ. Therefore, effective Forster energy transfer from PF backbone to DTQ1G and DTQ2G derivative would occur in the copolymer.

Fig. 3 showed the electrochemical properties of the polymers which were measured through cyclic voltammetry (CV). The highest occupied molecular orbital (HOMO) levels of polymers were calculated using the oxidation onset value of polymers and the

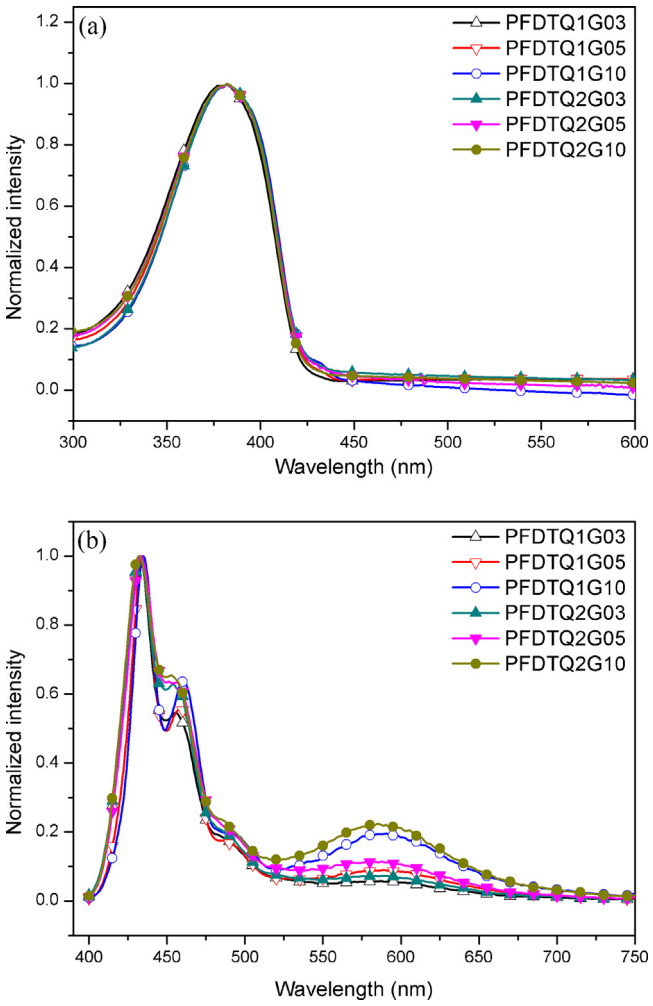

Fig. 1. (a) UV–vis absorption spectra and (b) PL emission spectra in thin film of polymers.

reference energy level (4.8 eV below the vacuum level) of ferrocene as follows:

$$\text{HOMO (eV)} = -4.8 - (E_{onset} - E_{1/2}(\text{Ferrocene})) \quad (1)$$

In contrast, the lowest unoccupied molecular orbital (LUMO) levels were estimated based on the difference between the HOMO level and the optical band gap calculated from UV–vis absorption onset value of polymer thin film. The HOMO and LUMO levels of the polymers and optical band gap are exhibited in Table 2.

The HOMO levels of all polymers were −5.85 to −5.89 eV and the LUMO levels were −2.90 to −2.94 eV, respectively. In terms of the HOMO and LUMO levels, all polymers were similar with PF, because the DTQ1G, DTQ2G dopant content was very small (0.1 mol% or less), having little effect on the polymer backbone [5]. The inset in Fig. 3 shows the energy band diagrams of PF, DTQ1G and DTQ2G derivative. As shown in these diagrams, the energy level of the DTQ1G, DTQ2G dopant exists between the HOMO and LUMO levels of PF. Thus, it was expected that charge trapping would effectively occur from PF to DTQ1G, DTQ2G [5,34].

5. Electroluminescence properties and current–voltage–luminance characteristics

Fig. 4 shows the electroluminescent spectra of the EL device. The brightness–voltage and efficiency–current density of the EL device are shown in Fig. 5(a) and (b), respectively, and their

Table 2
Optical and electrochemical properties of polymers.

Polymer	Solution, λ_{max} (nm)		Film, λ_{max} (nm)		E_{HOMO} (eV)	E_{LUMO} (eV)
	Absorption	Emission	Absorption	Emission		
PFDTQ1G03	382	417, 439	382	432, 587	5.89	2.94
PFDTQ1G05	385	417, 440	382	434, 589	5.89	2.94
PFDTQ1G10	385	417, 440	382	435, 591	5.89	2.94
PFDTQ2G03	384	417, 440	382	432, 590	5.87	2.92
PFDTQ2G05	384	417, 440	382	433, 588	5.88	2.93
PFDTQ2G10	384	417, 440	382	432, 586	5.85	2.90

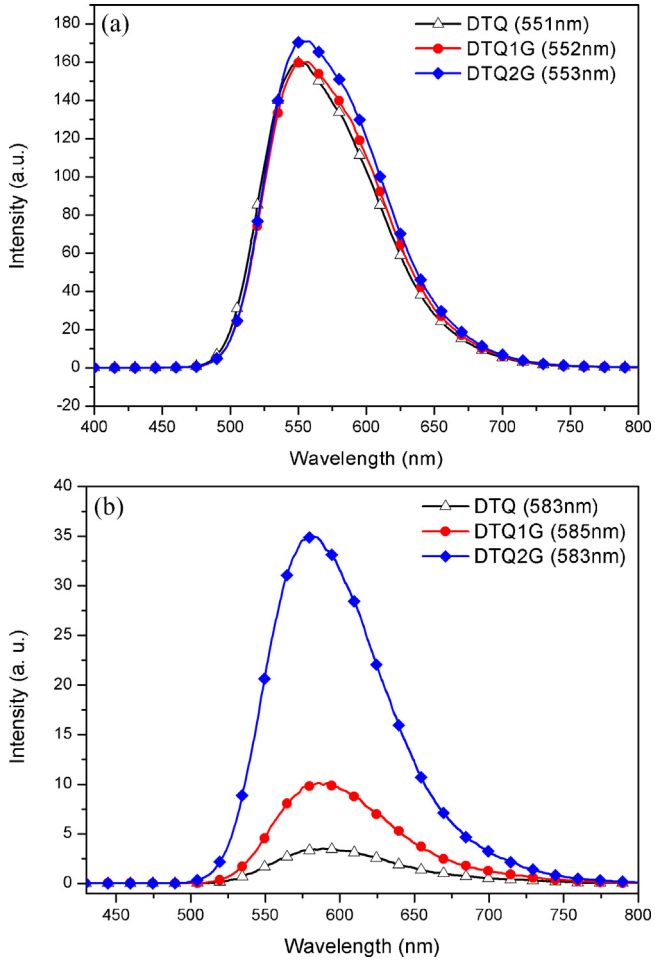

Fig. 2. Photoluminescent spectra of DTQ, DTQ1G, DTQ2G in (a) solution (10^{-5} M) and (b) thin film.

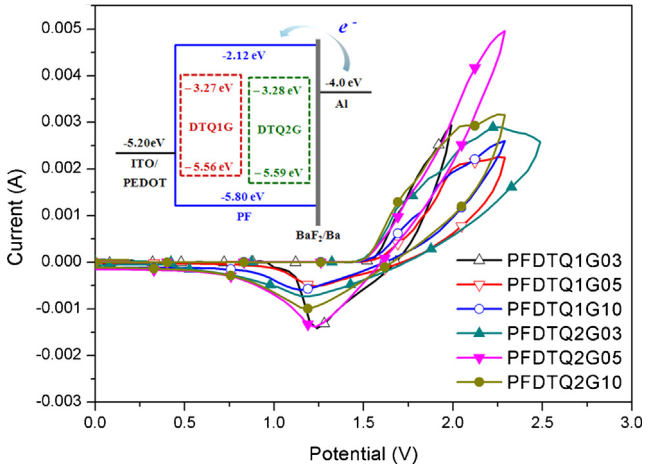

Fig. 3. Cyclic voltammogram of polymers and band diagram of PF, DTQ1G, DTQ2G.

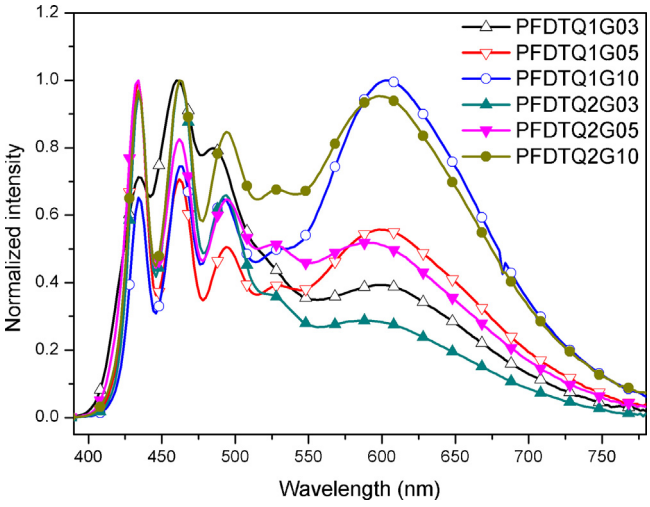

Fig. 4. Electroluminescent spectra of polymers.

characteristics are summarized in Table 3. The device was fabricated with ITO/PEDOT:PSS/polymer/BaF_2/Ba/Al structure, as shown in the inset of Fig. 5(a), and the emission layer was fabricated to 70–80 nm thickness through spin-coating.

In case of PFDTQ1G03, PFDTQ1G05 and PFDTQ1G10, emissions broadened at 550–650 nm as the DTQ1G derivative content increased, because of incomplete energy transfer from fluorene derivative to DTQ1G derivative. Furthermore, as DTQ1G derivative content increased, spectra intensity increased around 600 nm with similar pattern to the PL spectra. In similarly, in case of

Table 3
Summary of EL device performances of polymers.

Polymer	EL emission λ_{max} (nm)	Luminous efficiency (cd/A)	Power efficiency (lm/W)	Maximum brightness (cd/m^2)	CIE coordinate (x, y)
PFDTQ1G03	460, 598	0.23	0.10	817	(0.27, 0.26)
PFDTQ1G05	434, 598	0.55	0.21	2708	(0.33, 0.30)
PFDTQ1G10	464, 604	0.47	0.19	2920	(0.39, 0.35)
PFDTQ2G03	462, 588	0.66	0.29	3792	(0.25, 0.25)
PFDTQ2G05	434, 590	0.44	0.18	2238	(0.30, 0.30)
PFDTQ2G10	462, 598	0.46	0.19	2435	(0.35, 0.34)

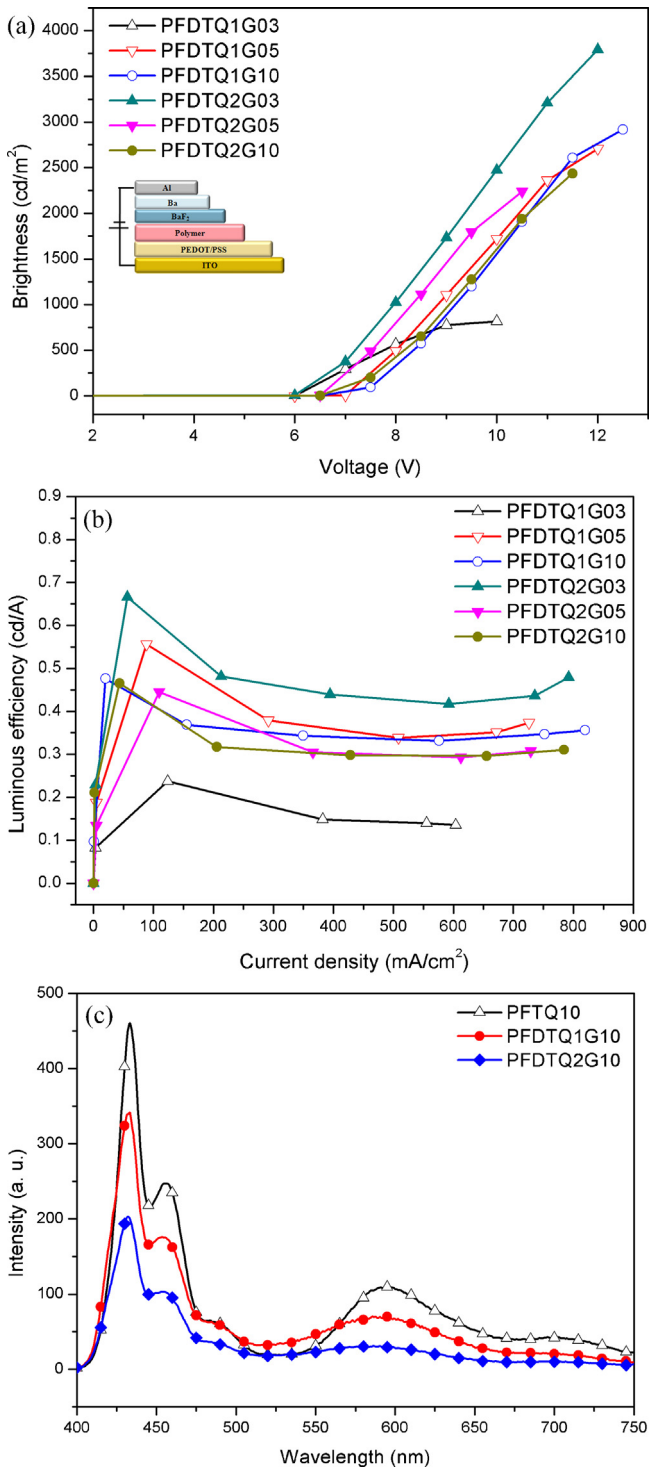

Fig. 5. (a) Voltage–brightness (*V–B*), (b) current density–luminous efficiency (*J–LE*) curves and (c) photoluminescent spectra of PFTQ10, PFDTQ1G10, PFDTQ2G10 in thin film (thickness 80 nm).

PFDTQ2G03, PFDTQ2G05 and PFDTQ2G10, emission spectra broadened at 550–650 nm.

Overall, differences were found between the PL spectra and EL spectra. Unlike in the PL spectra, similar intensity was found in orange-red emissions (λ_{max} = 598 nm) in the blue emission (λ_{max} = 434 nm) of the EL spectra. It has been confirmed that the low energy level of DTQ1G and DTQ2G derivative worked as a charge trapping site. This kind of result is matched with the HOMO and LUMO levels of the dopant confirmed in electrochemical measurements [5,19]. As shown in Table 3, the CIE coordinates of PFDTQ1G05 and PFDTQ2G10 were (0.33, 0.30) and (0.35, 0.34), respectively, which are close to the pure white coordinates of (0.33, 0.33).

The best EL performance was exhibited in PFDTQ2G03, which was observed with 0.66 cd/A luminous efficiency, 0.29 power efficiency (lm/W), 3792 cd/m^2 maximum brightness, and CIE coordinates of (0.25, 0.25). Stable luminous efficiency and the best performance occurred in PFDTQ2G03 because of the well-balanced electron and hole injection in the DTQ2G derivative ratio and effective energy transfer and charge trapping between fluorene and DTQ2G derivative [5,34].

Contrary to what was expected, the polymers containing DTQ1G and DTQ2G were not superior to the polymers without dendritic derivative despite amplified emission of DTQ1G, DTQ2G monomer compared with emission of alkyl chain quinoxaline [36]. This result may be because charge transportation was hindered by the dominant shielding effect of the fluorene backbone by dendritic bulky side chain [27,31]. To demonstrate shielding effect, photoluminescence spectra of PFDTQ1G10, PFDTQ2G10, PFTQ10 [35] were investigated as films cast (thickness: 80 nm) in the same condition. As shown in Fig. 5(c), it showed that PL intensities of PFDTQ1G10, PFDTQ2G10 were much lower compared to that of PFTQ10, which implies dendritic derivative exhibit dominant shielding effect of fluorene backbone.

6. Conclusions

We successfully synthesized white-emitting polymers containing dendritic derivative (DTQ1G, DTQ2G) on a PF backbone. The synthesized polymers showed good solubility and thermal stability. In case of PL spectra, as dendritic derivative content increased, the emission peak around 590 nm broadened, unlike in solution, because of increased intermolecular interaction among polymer main chains. In thin film, the intensities of the dendritic TQ monomers increased with the generation number of the dendrons, which are attributed to the peripheral bulky dendron units. In an EL device, PFDTQ2G03 had stable and superior performance, because the ratio of PF and dopant was well balanced between electron and hole injection in the device. The luminous efficiency, maximum brightness, and CIE coordinates of the device were 0.66 cd/A, 3792 cd/m^2, and (0.25, 0.25). The CIE coordinates of PFDTQ1G05 and PFDTQ2G10 were (0.33, 0.30) and (0.35, 0.34), respectively, which are close to the pure white coordinates of (0.33, 0.33).

Acknowledgment

This work was supported by the Konkuk University.

Appendix A. Supplementary data

Supplementary data associated with this article can be found, in the online version, at http://dx.doi.org/10.1016/j.synthmet.2014.01.019.

References

[1] J.H. Burroughes, D.D.C. Bradley, A.R. Brown, R.N. Marks, K. Mackay, R.H. Friend, et al., Light-emitting diodes based on conjugated polymers, Nature 347 (6293) (1990) 539–541.
[2] C. Ulbricht, B. Beyer, C. Friebe, A. Winter, U.S. Schubert, Adv. Mater. 21 (2009) 4418–4441.
[3] H.J. Song, J.Y. Lee, I.S. Song, D.K. Moon, J.R. Haw, J. Ind. Eng. Chem. 17 (2011) 352–357.
[4] M. Kijima, I. Kinoshita, T. Hattori, H. Shirakawa, Synth. Met. 100 (1999) 61–69.
[5] H.J. Song, D.H. Kim, T.H. Lee, D.K. Moon, Eur. Polym. J. 48 (2012) 1485–1494.
[6] H. Wu, L. Ying, W. Yang, Y. Cao, Chem. Soc. Rev. 38 (2009) 3391–3400.

[7] A. Gadisa, W. Mammo, L.M. Andersson, S. Admassie, F. Zhang, L. Chen, M.R. Andersson, O. Inganäs, Adv. Funct. Mater. 23 (2007) 3836–3842.
[8] E. Wang, L. Hou, Z. Wang, S. Hellström, F. Zhang, O. Inganäs, M.R. Andersson, Adv. Mater. 22 (2010) 5240–5244.
[9] H.J. Song, D.H. Kim, E.J. Lee, D.K. Moon, J. Mater. Chem. A 1 (2013) 6010–6020.
[10] J.Y. Lee, A.N. Aleshin, D.W. Kim, H.J. Lee, Y.S. Kim, G. Wegner, V. Enkelmann, S. Roth, Y.W. Park, Synth. Met. 152 (2005) 169–172.
[11] I. Mcculloch, M. Heeney, C. Bailey, K. Genevicius, I. Macdonald, M. Shkunov, D. Sparrowe, S. Tierney, R. Wagner, W. Zhang, M.L. Chabinyc, R.J. Kline, M.D. Mcgehee, M.F. Toney, Nat. Mater. 5 (2006) 328–333.
[12] I. Osaka, M. Shimawaki, H. Mori, I. Doi, E. Miyazaki, T. Koganezawa, K. Takimiya, J. Am. Chem. Soc. 134 (2012) 3498–3507.
[13] M. Goh, S. Matsushita, K. Akagi, Chem. Soc. Rev. 39 (2010) 2466–2476.
[14] M.M. Alam, S.A. Jenekhe, Chem. Mater. 14 (2002) 4775–4780.
[15] J.H. Burroughes, D.D.C. Bradley, A.R. Brown, R.N. Marks, K. Mackay, R.H. Friend, P.L. Burns, A.B. Holmes, Nature 347 (1990) 539–541.
[16] Q. Pei, Y. Yang, J. Am. Chem. Soc. 118 (1996) 7416–7417.
[17] Z.a. Tan, R. Tang, E. Zhou, Y. He, C. Yang, F. Xi, Y. Li, J. Appl. Polym. Sci. 107 (2008) 514–521.
[18] X.Y. Deng, W.M. Lau, K.Y. Wong, K.H. Low, H.F. Chow, Y. Cao, Appl. Phys. Lett. 84 (2004) 3522–3524.
[19] M.J. Park, J.H. Lee, I.H. Jung, J.H. Park, D.H. Hwang, H.K. Shim, Macromolecules 41 (2008) 9643–9649.
[20] Q. Hou, Y. Xu, W. Yang, M. Yuan, J. Peng, Y. Cao, J. Mater. Chem. 12 (2002) 2887–2892.
[21] M. Sun, Q. Niu, B. Du, J. Peng, W. Yang, Y. Cao, Macromol. Chem. Phys. 208 (2007) 988–993.
[22] E. Xu, H. Zhong, H. Lai, D. Zeng, J. Zhang, W. Zhu, Q. Fang, Macromol. Chem. Phys. 211 (2010) 651–656.
[23] A. Tsami, X.H. Yang, F. Galbrecht, T. Farrell, H. Li, S. Adamczyk, R. Heiderhoff, L.J. Balk, D. Neher, E. Holder, J. Polym. Sci. A: Polym. Chem. 45 (2007) 4773–4785.
[24] Y.K. Lee, Y.M. Nam, W.H. Jo, J. Mater. Chem. 21 (2011) 8583–8590.
[25] N. Blouin, A. Michaud, D. Gendron, S. Wakim, E. Blair, R. Neagu-Plesu, M. Belletête, G. Durocher, Y. Tao, M. Leclerc, J. Am. Chem. Soc 130 (2008) 732–742.
[26] C.W. Wu, H.H. Sung, H.C. Lin, J. Polym. Sci. A: Polym. Chem. 23 (2006) 6765–6774.
[27] C.W. Wu, C.M. Tsai, H.C. Lin, Macromolecules 39 (2006) 4298–4305.
[28] D. Gedefaw, Y. Zhou, S. Hellstrom, L. Lindgren, L.M. Andersson, F. Zhang, J. Mater. Chem. 30 (2009) 5359–5363.
[29] Y.S. Kho, K.J. Roh, J.R. Haw, W.D. Jang, Y.J. Kim, M.S. Choi, J. Porphyrins Phthalocyanines 13 (2009) 769–773.
[30] B.Y. Hsieh, Y. Chen, J. Polym. Sci. A: Polym. Chem. 47 (2009) 833–844.
[31] H.J. Song, S.M. Lee, J.Y. Lee, B.H. Choi, D.K. Moon, Synth. Met. 161 (2011) 2451–2459.
[32] J. Xu, Y. Zhang, J. Hou, Z. Wei, S. Pu, J. Zhao, Eur. Polym. J. 42 (2006) 1154–1163.
[33] M. Fukuda, K. Sawada, K. Yoshino, J. Polym. Sci. A: Polym. Chem. 31 (1993) 2465–2471.
[34] Q. Chen, N. Liu, L. Ying, W. Yang, H. Wu, W. Xu, Polymer 50 (2009) 1430–1437.
[35] J. Wang, Y. Zhao, C. Dou, H. Sun, P. Xu, K. Ye, J. Zhang, S. Jiang, F. Li, Y. Wang, J. Phys. Chem. 111 (2007) 5082–5089.
[36] M.H. Han, H.J. Song, T.H. Lee, J.Y. Lee, D.K. Moon, J.R. Haw, Synth. Met. 162 (2012) 2294–2301.